Astron. Astrophys. 358, 665–670 (2000)

ASTRONOMY AND ASTROPHYSICS

Dust cloud formation in stellar environments

I. A radiative/thermal instability of dust forming gases

P. Woitke[1], **E. Sedlmayr**[1], **and B. Lopez**[2]

[1] TU Berlin, Institut für Astronomie und Astrophysik, Sekr. PN 8-1, Hardenbergstrasse 36, 10623 Berlin, Germany
[2] Observatoire de la Côte d'Azur, Département Fresnel UMR 6528, B.P. 4229, 06034 Nice Cedex 4, France

Received 24 February 2000 / Accepted 13 April 2000

Abstract. In this paper, we report on an instability possibly inherent in dust forming media due to multi-dimensional radiative transfer effects. Starting from a solution of a grey 1D or 2D radiative transfer problem, we introduce small harmonic 3D-perturbations of the opacity structure $\kappa(\boldsymbol{r})$ and show that, in the linear approximation, the mean intensity $J(\boldsymbol{r})$ is modified in the same manner, resulting in spatial variations of the temperature structure. If the medium possesses a strongly temperature-dependent opacity – as expected in dust forming environments – the perturbations can be self-amplifying. We apply this concept to a spherically symmetric, stationary model for the dust-driven wind of IRC+10216 and find that large-scale perturbation modes perpendicular to the radial direction are unstable in the outer parts of the dust formation region ($r \gtrsim 2.5\,R_*$), which may result in the formation of dust clouds.

Key words: instabilities – radiative transfer – ISM: dust, extinction – stars: late-type – stars: circumstellar matter – stars: individual: IRC+10216

1. Introduction

Recent observations with high angular resolution have accumulated convincing evidence that dust forming objects like the outflows of AGB stars, novae and supernovae ejecta, the hot winds of Wolf-Rayet stars or the outer atmospheres of R Coronae Borealis stars often exhibit a clumpy circumstellar environment. Prominent examples are the irregular, cloudy structures in the inner part of the circumstellar envelope of the infrared carbon star IRC+10216 (Weigelt et al. 1998; Haniff & Buscher 1998; Tuthill et al. 2000), and the patchy SiO maser spots inside the wind acceleration zone of the oxygen-rich Mira variable TX Cam (Diamond & Kemball 1999). A summary and discussion of such observations concerning AGB and post-AGB stars can be found e. g. in Lopez (1999).

The question arises whether the observed clumpiness of dusty media is simply a manifestation of pre-existing inhomogeneities or asymmetries in the condensing outflows (which merely become visible via dust formation), or whether the dust formation process itself introduces new and significant instabilities to the medium which cause the structure formation. In this paper we investigate the second possibility.

Send offprint requests to: P. Woitke (woitke@physik.tu-berlin.de)

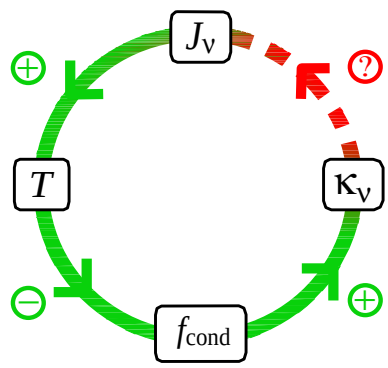

Fig. 1. Control loop of interactions in a dust forming system. Positive feedbacks are marked by $\oplus$, negative feedbacks by $\ominus$. The sign of the feedback marked by the dashed arrow (non-local effect of opacity changes on the mean intensity) determines whether the control loop is self-amplifying, or whether it damps initial perturbations.

As will be argued below, a control loop of physical interactions can be identified in dust forming gases, where the non-local coupling via radiative transfer plays a crucial role. Investigations on similar radiative/thermal instabilities have been carried out by Spiegel (1957) and Trujillo Bueno & Kneer (1990). These works have mainly considered short-time, small-scale perturbations of stellar atmospheres in the diffusion limit, in particular concerning the sun. In this paper, we are interested in possible large-scale structure formation processes in the outflows of red giants, where a new and extremely temperature-sensitive source of opacity arises (the dust) which is exposed to directed, radially diluted star light.

2. The nature of the instability

We consider radiative/thermal instabilities in a dust forming system as illustrated in Fig. 1. The following assumptions on the important interactions in the system are made:

1. A decrease/increase of the local mean intensity J_ν causes a decrease/increase of the local temperature in the dust form-

ing medium T (positive feedback), as it is always true in radiative equilibrium.
2. A decrease of the temperature T improves the conditions for dust formation and, thereby, leads to an increase of the degree of condensation $f_{\rm cond}$ (negative feedback).
3. An increase of the degree of condensation $f_{\rm cond}$ causes an increase of the opacity κ_ν (positive feedback).

As will be discussed in Sect. 3, an increase of the opacity κ_ν may either cause a decrease (negative feedback) or an increase (positive feedback) of the mean intensity J_ν via radiative transfer effects, depending on the circumstances. In any case, a control loop is constituted (see Fig. 1) which acts on relatively short time scales, where the slowest process inside the loop likely is the dust formation (see Sect. 5). If the latter influence is negative, the overall feedback in the control loop is positive ($\oplus\cdot\ominus\cdot\oplus\cdot\ominus = \oplus$). In such a case the control loop is self-amplifying, i. e. unstable against small perturbations which may arise e. g. from fluctuations. This kind of instability possibly causes a spatial structuring of the dust forming medium. In the opposite case, initial perturbations are damped by the dust forming system. According to the assumptions outlined, the stability of dust forming regions is hence controlled by the non-local effect of opacity variations on the mean intensity, which is investigated below.

3. Radiative transfer in a perturbed medium

3.1. Basic form of the radiative transfer equation

We consider the time-independent equation of radiative transfer with coherent, isotropic scattering along a ray in direction of the unit vector $\boldsymbol{n}$

$$-\frac{dI_\nu(\boldsymbol{r},\boldsymbol{n})}{ds} = -\left[\kappa_\nu^{\rm abs}(\boldsymbol{r})+\sigma_\nu(\boldsymbol{r})\right] I_\nu(\boldsymbol{r},\boldsymbol{n}) + \kappa_\nu^{\rm abs}(\boldsymbol{r}) S_\nu(\boldsymbol{r}) + \sigma_\nu(\boldsymbol{r}) J_\nu(\boldsymbol{r}) \,. \quad (1)$$

$I_\nu(\boldsymbol{r},\boldsymbol{n})$ is the intensity at the point $\boldsymbol{r}$ in direction $\boldsymbol{n}$ at frequency ν, $J_\nu(\boldsymbol{r}) = 1/(4\pi)\int I_\nu(\boldsymbol{r},\boldsymbol{n})\,d\Omega$ the mean intensity, $S_\nu(\boldsymbol{r})$ the source function, $\kappa_\nu^{\rm abs}(\boldsymbol{r})$ the true absorption coefficient and $\sigma_\nu(r)$ the scattering coefficient. The negative sign on the l.h.s. of Eq. (1) is because of the definition of s, which denotes the distance backward along the ray $\boldsymbol{r} = \boldsymbol{r}_0 - s\,\boldsymbol{n}$ (Mihalas & Weibel Mihalas 1984, p. 345).

The following basic assumptions are made: grey transport coefficients $\kappa_\nu^{\rm abs} = \kappa^{\rm abs}$, $\sigma_\nu = \sigma$, and radiative equilibrium $\int \kappa_\nu^{\rm abs} J_\nu\, d\nu = \int \kappa_\nu^{\rm abs} S_\nu\, d\nu$. Frequency-integration of Eq. (1) in this case yields

$$-\frac{dI(\boldsymbol{r},\boldsymbol{n})}{ds} = \kappa(\boldsymbol{r})\left[J(\boldsymbol{r}) - I(\boldsymbol{r},\boldsymbol{n})\right] , \quad (2)$$

where $\kappa = \kappa^{\rm abs} + \sigma$ is the grey opacity of the medium and I and J are the respective frequency-integrated quantities. The formal solution of Eq. (2) is

$$I(\boldsymbol{r}_0,\boldsymbol{n}) = I(\boldsymbol{r}_0 - s_{\rm max}\boldsymbol{n},\boldsymbol{n})\,{\rm e}^{-\tau(\boldsymbol{r}_0,\boldsymbol{n},s_{\rm max})} + \int_0^{s_{\rm max}} \kappa(\boldsymbol{r})\,J(\boldsymbol{r})\,{\rm e}^{-\tau(\boldsymbol{r}_0,\boldsymbol{n},s)}\,ds \quad (3)$$

with the optical depth being defined as

$$\tau(\boldsymbol{r}_0,\boldsymbol{n},s) = \int_0^s \kappa(\boldsymbol{r}_0 - s'\boldsymbol{n})\,ds' \,. \quad (4)$$

The integration in Eq. (3) is carried out from the starting point $\boldsymbol{r}_0$ $(s=0)$ backward along the ray to the maximum distance $s_{\rm max} = s_{\rm max}(\boldsymbol{r}_0,\boldsymbol{n})$ where the ray enters the considered volume. This may occur either at an outer boundary, where the irradiation is assumed to be zero, or at an inner boundary where the incident intensity $I(\boldsymbol{r}_0 - s_{\rm max}\boldsymbol{n},\boldsymbol{n})$ is considered to be known. By integration of Eq. (3) over the solid angle, the following basic form of the radiative transfer equation is obtained:

$$J(\boldsymbol{r}_0) = \frac{1}{4\pi}\iint I(\boldsymbol{r}_0 - s_{\rm max}\boldsymbol{n},\boldsymbol{n})\,{\rm e}^{-\tau(\boldsymbol{r}_0,\boldsymbol{n},s_{\rm max})}\,d\Omega + \frac{1}{4\pi}\iint\int_0^{s_{\rm max}} \kappa(\boldsymbol{r})\,J(\boldsymbol{r})\,{\rm e}^{-\tau(\boldsymbol{r}_0,\boldsymbol{n},s)}\,ds\,d\Omega \quad (5)$$

3.2. Consideration of perturbations

We consider a solution of the radiative transfer problem Eq. (5) $\{\kappa_0(\boldsymbol{r}), J_0(\boldsymbol{r})\}$, which has been calculated by means of simplifying assumptions concerning the geometry. For example, such an unperturbed problem can be a standard plane-parallel stellar atmosphere (1D), a spherically symmetric stellar wind (1D), or an axisymmetric radiative transfer problem (2D). Next, we introduce small, three-dimensional, harmonic perturbations[1] of the spatial opacity and mean intensity structures

$$\kappa(\boldsymbol{r}) = \kappa_0(\boldsymbol{r})\left(1 + \delta\kappa\cdot{\rm e}^{i(\boldsymbol{k}\cdot\boldsymbol{r}+\delta)}\right) \quad (6)$$

$$J(\boldsymbol{r}) = J_0(\boldsymbol{r})\left(1 + \delta J\cdot{\rm e}^{i(\boldsymbol{k}\cdot\boldsymbol{r}+\delta)}\right) , \quad (7)$$

where $\delta\kappa \ll 1$ and $\delta J \ll 1$ are the (constant) relative amplitudes of the perturbations which are assumed to be small. The wave vector $\boldsymbol{k}$ describes the wavelength and the direction of the perturbation ($|k| = 2\pi/\lambda$). The incident intensities are assumed to be unaffected by the perturbations $I(\boldsymbol{r}_0 - s_{\rm max}\boldsymbol{n},\boldsymbol{n}) = I_0(\boldsymbol{r}_0 - s_{\rm max}\boldsymbol{n},\boldsymbol{n})$.

Strictly speaking, we assume a perturbation of $\kappa(\boldsymbol{r})$ as expressed by Eq. (6) and will show that the ansatz for the response of the radiation field (Eq. 7) leads to non-trivial solutions of Eq. (5).

By inserting Eq. (6) into (4), the optical depth in the perturbed medium is

$$\tau(\boldsymbol{r}_0,\boldsymbol{n},s) = \int_0^s \kappa_0(\boldsymbol{r}_0 - s'\boldsymbol{n})\left(1 + \delta\kappa\,{\rm e}^{i(\boldsymbol{k}\cdot\boldsymbol{r}_0 - s'\boldsymbol{k}\cdot\boldsymbol{n}+\delta)}\right)ds' = \tau_0(\boldsymbol{r}_0,\boldsymbol{n},s) + \delta\kappa\int_0^s \kappa_0(\boldsymbol{r}_0 - s'\boldsymbol{n})\,{\rm e}^{i(a+bs')}\,ds' \,, \quad (8)$$

[1] Since time-independent radiative transfer and radiative equilibrium is assumed (see Eq. 2), the time t can be considered as fixed and the phase is defined as $\delta = \delta' - i\omega t$ from the usual expression for plane waves ${\rm e}^{i(\boldsymbol{k}\cdot\boldsymbol{r}-\omega t+\delta')}$.

with $\tau_0(\boldsymbol{r}_0,\boldsymbol{n},s) = \int_0^s \kappa_0(\boldsymbol{r}_0 - s'\boldsymbol{n})\,ds'$ being the respective optical depth in the unperturbed medium and where $a = \boldsymbol{k}\cdot\boldsymbol{r}_0 + \delta$ and $b = -\boldsymbol{k}\cdot\boldsymbol{n}$ are abbreviations. Since $\delta\kappa \ll 1$, we find to first order

$$\mathrm{e}^{-\tau(\boldsymbol{r}_0,\boldsymbol{n},s)} \approx \mathrm{e}^{-\tau_0(\boldsymbol{r}_0,\boldsymbol{n},s)}\left(1 - \delta\kappa \int_0^s \kappa_0\,\mathrm{e}^{i(a+bs')}\,ds'\right) \tag{9}$$

Insertion of Eqs. (6), (7) and (9) into Eq. (5) and truncation to first order terms yields

$$\begin{aligned} J_0(\boldsymbol{r}_0)\left(1+\delta J\,\mathrm{e}^{ia}\right) &\approx \qquad (10)\\ \approx\ & \frac{1}{4\pi}\iint I_0\,\mathrm{e}^{-\tau_0}\left[1-\delta\kappa\int_0^{s_{\max}}\kappa_0\,\mathrm{e}^{i(a+bs)}\,ds\right]d\Omega\\ &+\frac{1}{4\pi}\iint\int_0^{s_{\max}}\kappa_0\,J_0\,\mathrm{e}^{-\tau_0}\left[1+(\delta\kappa+\delta J)\,\mathrm{e}^{i(a+bs)}\right]ds\,d\Omega\\ &-\frac{1}{4\pi}\iint\int_0^{s_{\max}}\kappa_0\,J_0\,\mathrm{e}^{-\tau_0}\delta\kappa\left(\int_0^s\kappa_0\,\mathrm{e}^{i(a+bs')}ds'\right)ds\,d\Omega \end{aligned}$$

where the arguments of $I_0 = I_0(\boldsymbol{r}_0 - s_{\max}\boldsymbol{n},\boldsymbol{n})$, $J_0 = J_0(\boldsymbol{r})$, $\kappa_0 = \kappa_0(\boldsymbol{r})$ and $\tau_0 = \tau_0(\boldsymbol{r}_0,\boldsymbol{n},s)$ have been omitted. Remembering that $\{\kappa_0(\boldsymbol{r}), J_0(\boldsymbol{r})\}$ satisfies Eq. (5), the 0th order of Eq. (10) cancels out as well as the constant factor e^{ia}. The latter means that the amplitude of the mean intensity variation δJ is in fact phase-independent and that there is no phase-shift between the opacity and the mean intensity variation. After separating the remainder of Eq. (10) into terms containing only $\delta\kappa$ and δJ, respectively, the following result for the ratio of perturbation amplitudes can be obtained

$$\frac{\delta J}{\delta\kappa} = \frac{\mathcal{A}_1(\boldsymbol{r}_0,\boldsymbol{k}) - \mathcal{A}_2(\boldsymbol{r}_0,\boldsymbol{k}) - \mathcal{A}_3(\boldsymbol{r}_0,\boldsymbol{k})}{J_0(\boldsymbol{r}_0) - \mathcal{A}_1(\boldsymbol{r}_0,\boldsymbol{k})} \tag{11}$$

with the abbreviations

$$\mathcal{A}_1(\boldsymbol{r}_0,\boldsymbol{k}) = \frac{1}{4\pi}\iint\int_0^{s_{\max}}\kappa_0\,J_0\,\mathrm{e}^{-\tau_0}\,\mathrm{e}^{ibs}\,ds\,d\Omega \tag{12}$$

$$\mathcal{A}_2(\boldsymbol{r}_0,\boldsymbol{k}) = \frac{1}{4\pi}\iint\int_0^{s_{\max}}\kappa_0\,J_0\,\mathrm{e}^{-\tau_0}\left(\int_0^s\kappa_0\,\mathrm{e}^{ibs'}ds'\right)ds\,d\Omega \tag{13}$$

$$\mathcal{A}_3(\boldsymbol{r}_0,\boldsymbol{k}) = \frac{1}{4\pi}\iint I_0\,\mathrm{e}^{-\tau_0}\left(\int_0^{s_{\max}}\kappa_0\,\mathrm{e}^{ibs}\,ds\right)d\Omega\,. \tag{14}$$

The resultant ratio of the perturbation amplitudes $\delta J/\delta\kappa$ depends on the overall spatial structure of the unperturbed solution $\{\kappa_0(\boldsymbol{r}), J_0(\boldsymbol{r})\}$, and on $\boldsymbol{r}_0$ and $\boldsymbol{k}$. It is noteworthy that linear-combinations of opacity perturbations in different directions and with different amplitudes $\kappa_0(\boldsymbol{r})\cdot(1+\sum\delta\kappa_j\,\mathrm{e}^{i(\boldsymbol{k}_j\cdot\boldsymbol{r}+\delta_j)})$ result in the same type of mean intensity perturbations $J_0(\boldsymbol{r})\cdot(1+\sum\delta J_j\,\mathrm{e}^{i(\boldsymbol{k}_j\cdot\boldsymbol{r}+\delta_j)})$ where Eqs. (11) to (14) remain valid for each single mode $\delta J_j/\delta\kappa_j(\boldsymbol{r}_0,\boldsymbol{k}_j)$.

In comparison to the results of Spiegel (1957) and Trujillo Bueno & Kneer (1990), the presented formalism (11) to (14) is applicable to arbitrary points and geometries of the unperturbed problem, since it does not rely on the diffusion approximation and accounts for incident radiation fields.

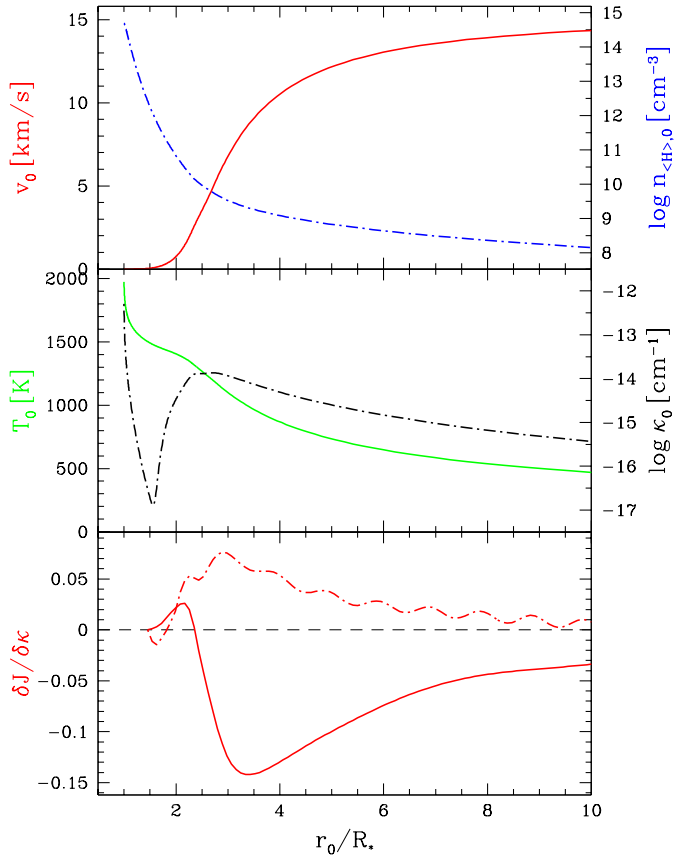

Fig. 2. Results of the perturbed radiative transfer in application to a spherical symmetric, stationary, dust-driven wind model for IRC+10216. The upper two plots show the unperturbed model: velocity (upper panel, full line), density (upper panel, dashed line), temperature (middle panel, full line) and total (gas + dust) opacity (middle panel, dashed line). The lower plot shows the calculated ratio of perturbation amplitudes between the mean intensity and the opacity for two perturbation modes $\boldsymbol{k}\perp\boldsymbol{r}_0$, $\lambda = 1\,R_*$ (full line) and $\boldsymbol{k}\parallel\boldsymbol{r}_0$, $\lambda = 1\,R_*$ (dashed line). According to the arguments outlined in Sect. 2, $\delta J/\delta\kappa > 0$ indicates stability whereas $\delta J/\delta\kappa < 0$ indicates instability.

4. Results

Eqs. (11) to (14) form a complete set of algebraic expressions which allows for the calculation of the response of the radiation field to small harmonic (3D) perturbations of the grey opacity structure in radiative equilibrium. As argued in Sect. 2, the ratio of the perturbation amplitudes $\delta J/\delta\kappa$ controls the stability of the dust formation zone. In the following, we apply this concept to discuss possible structure formation processes in stationary, dusty winds of AGB stars.

For the unperturbed solution $\{\kappa_0(\boldsymbol{r}), J_0(\boldsymbol{r})\}$ we use the results of a spherically symmetric, self-consistent, grey, dust-driven wind model provided by Dominik et al. (1990), which is shown in Fig. 2. The model is determined by four parameters which have been chosen as follows: stellar mass $M_* = 0.7 M_\odot$, stellar luminosity $L_* = 2.5\cdot 10^4 L_\odot$, mass loss rate $\dot{M} = 8\cdot 10^{-5} M_\odot/\mathrm{yr}$, and carbon-to-oxygen ratio $\mathrm{C/O} = 1.4$. Besides the velocity, density, temperature and dust structure, the

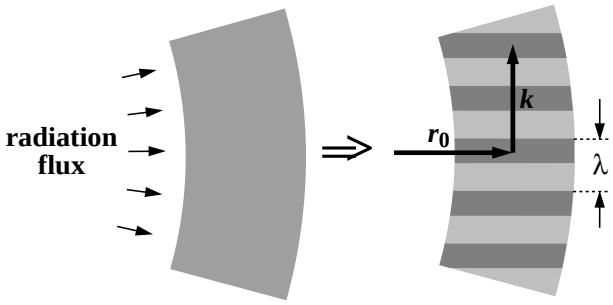

Fig. 3. Geometry of the considered perpendicular perturbation mode $\boldsymbol{k} \perp \boldsymbol{r}_0$. A part of a homogeneous dust shell is depicted on the l.h.s. The r.h.s. shows the same part under the influence of the perturbation.

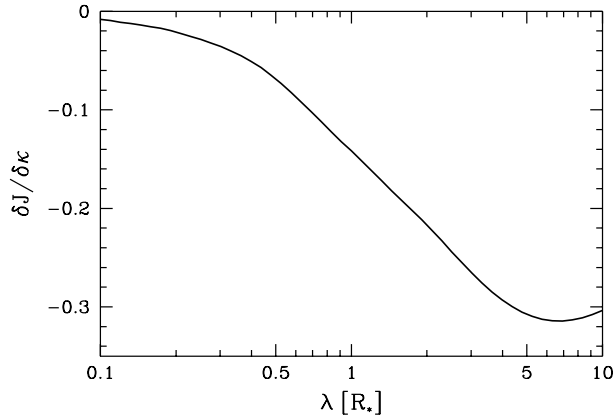

Fig. 4. Influence of the wavelength λ of the perpendicular perturbation ($\boldsymbol{k} \perp \boldsymbol{r}_0$, $|k| = 2\pi/\lambda$) on the calculated ratio of perturbation amplitudes at fixed radial distance $|r_0| = 3.4\,R_*$.

stellar temperature ($T_* = 1975$ K) and the final outflow velocity ($v_\infty = 15.3$ km/s) are results of the model calculation. This model has been used as the initial model for the more sophisticated iteration procedure required to construct a self-consistent, stationary, frequency-dependent model for the infrared carbon star IRC+10216 by Winters et al. (1994), who found the best agreement with the observations for the upper choice of parameters.

No special numerical technique was required to compute the integrals in Eqs. (12) to (14). A simple nested integration scheme according to Simpson's rule has been applied with 80×80 angular and typically 40 to 200 spatial grid points along the discrete rays, using local spherical coordinates. In order to avoid spurious effects caused by an unintended perturbation of the stellar photosphere, the inner boundary is placed at $1.5\,\mathrm{R}_*$, i. e. well inside the dust shell. The results are shown in the lower part of Fig. 2 for two exemplarily chosen perturbation modes.

Perturbations along the radial direction ($\boldsymbol{k} \parallel \boldsymbol{r}_0$) are generally found to be characterized by $\delta J/\delta\kappa > 0$. The behavior of these modes is similar to radial perturbations in spherical symmetry: A shell-like increase of the grey opacity does not affect the bolometric flux at any point (which is fixed by the stellar luminosity and the radius), but only hinders and dams the outflowing radiation. Thereby, the mean intensity is increased inside of the point of increased opacity (backwarming)[2]. This dependence is evident from the monotonically increasing $J(\tau)$-relation in grey stellar atmospheres (e. g. Mihalas 1978, p. 55). According to the arguments given in Sect. 2, such perturbations are stable in the dust formation zone. The slight, periodical variations of δJ as a function of distance arise from the phase-relation between the point of interest $\boldsymbol{r}_0$ and the point of maximum opacity in the dust shell which mainly contributes to the local mean intensity at $\boldsymbol{r}_0$.

Perturbation modes perpendicular to the radial direction ($\boldsymbol{k} \perp \boldsymbol{r}_0$) behave in a different way. A perpendicular perturbation of the dust formation zone, located between about $2\,\mathrm{R}_*$ and $4\,\mathrm{R}_*$ in the model with corresponding optical depth $\Delta\tau \approx 2.3$, introduces a tendency to decompose the dust shell into several fragments (here equidistant slabs of size $\lambda/2$, see Fig. 3). In a medium of this kind, the flux preferentially escapes through the "holes" in the shell, which at the same time increases the mean intensity between and decreases the mean intensity inside the slabs. Accordingly, locations with increased opacity coincide with locations of decreased intensity $\delta J/\delta\kappa < 0$.

Analysis of the full $\delta J/\delta\kappa$-curve in Fig. 2 reveals that actually both effects mentioned above are active in the case $\boldsymbol{k} \perp \boldsymbol{r}_0$. At the inner edge of the dust shell ($r \lesssim 2.5\,R_*$) the backwarming effect dominates and $\delta J/\delta\kappa > 0$. For larger radial distances (about outside of the point of maximum $\kappa_0(r_0)$ in Fig. 2, which approximately coincides with the sonic point in the model) the formation of flux tubes and in-between situated shadowed regions as sketched in Fig. 3 is more significant and $\delta J/\delta\kappa < 0$. As discussed in Sect. 2, the dust formation will be accelerated in the shadowed, cooler regions and the opacity contrast will increase. Thus, the perpendicular perturbation mode is found to be self-amplifying beyond some critical distance (here $r \gtrsim 2.5\,R_*$).

Fig. 4 illustrates the influence of the wavelength λ of the perpendicular κ-perturbation on the resulting δJ amplitude. As apparent from the figure, $\lambda \gtrsim 1\,R_*$ is required to cause noticeable changes of the radiation field. Otherwise, the medium is essentially optically thin within the perturbations and the small-scale variations have no profound effect in the radiative transfer, since they cannot accumulate sufficient optical depth across one perturbation length λ. A saturation of $\delta J/\delta\kappa$ can be noted at $\lambda \approx 6\,R_*$, possibly because such perturbation modes already cover the entire dust formation zone in the model.

5. Discussion

The main intention of this paper is to identify an instability which might initiate structure formation in dust forming media. We have considered a control loop of physical interactions which can be self-amplifying under certain circumstances. One remaining question in this context is, whether the chosen interactions depicted in Fig. 1 do in fact form a tightly coupled

[2] The backwarming effect may be overestimated in the grey approximation, because the thermal re-emission of the dust preferentially takes place at longer wavelengths where the photons have a larger probability to escape.

"closed" loop, where the internal perturbations have sufficient time to grow disregarding outer influences, or whether the chosen subset of feedbacks strongly interferes with other physical interactions not taken into account like the expansion of the system in the wind flow. In order to discuss the degree of coupling among the various interactions, we estimate some characteristic time scales in the following.

Radiative transfer time scale. The free travel time for photons crossing the dust shell is $\Delta r/c \approx 5$ hours for $\Delta r = 6\,R_*$. The photon diffusion time scale, which accounts for multiple absorption/reemission and scattering events, should not exceed this time by a large factor since the optical depths in the dust shell are of the order of unity. Hence, local changes of the opacity almost immediately affect the mean intensity structure in the entire part of the considered circumstellar envelope.

Radiative cooling time scale. This time scale determines how fast changes of J transform into changes of T. Assuming a thermally coupled, dusty gas in LTE, the relaxation time scale towards radiative equilibrium $\left(\frac{4\pi\widehat{\kappa}}{c_V}\frac{\partial B}{\partial T}\right)^{-1}$is as short as $50\ \mathrm{sec}$, where $\widehat{\kappa} \approx 1.5\ \mathrm{cm}^2\,\mathrm{g}^{-1}$ is the total (dust + gas) opacity per mass at $3\,R_*$ and $c_V \approx 9\cdot 10^7 \mathrm{erg\,K^{-1}g^{-1}}$ is the heat capacity of the predominantly neutral, H_2-rich gas. This short radiative cooling time scale enables us to assume radiative equilibrium in Sect. 3, even under the influence of the perturbations. However, thermal coupling between dust and gas is questionable. Realistic cooling time scales for the decoupled dust component may be as short as 0.01 sec (Woitke 2000). In contrast, the cooling time scale for the gas component may be as long as days, weeks or even months, mainly driven by molecular line cooling under non-LTE conditions (Woitke et al. 1996).

Chemical time scale. The formation of molecules accelerates the radiative cooling of the gas via the formation of new important coolants (e. g. CO, CS and HCN in the carbon-rich case) and provides the basic progenitor molecules for dust formation (e. g. C_2H_2). The characteristic time scale for the formation of these molecules is rather uncertain and may vary strongly among the molecules. Patzer et al. (1999) have shown that neutral-neutral reactions in the circumstellar envelopes of pulsating red giants already fail to maintain chemical equilibrium relatively close to the star ($T \approx 2000\,\mathrm{K}$, $n_{<\mathrm{H}>} \approx 5\cdot 10^{10}\mathrm{cm}^{-3}$). At lower temperatures/densities, the chemical time scale exceeds the hydrodynamical expansion time scale and the chemistry is found to be frozen in. Neufeld & Hollenbach (1994) have investigated the time-dependent chemistry of a 50 km/s accretion shock wave propagating into a predominantly neutral $10^9\mathrm{cm}^{-3}$ gas. The shock wave initially destroys virtually all molecules and compresses the gas up to a few $10^{11}\mathrm{cm}^{-3}$. Molecules like H_2, CO, H_2O and OH were found to be re-formed after about 5 days. It has been argued that the chemical time scale must be significantly smaller than the dust formation time scale, because the dust nucleation is a chemical process which requires many reaction steps (Gail & Sedlmayr 1988).

Dust formation time scale. The formation of dust usually introduces the longest internal time scale to astrophysical gases. According to the dust formation theory developed by Gail et al. (1984) and Gail & Sedlmayr (1988), typical dust formation time scales in stellar winds are found to be of the order of a few months in the carbon-rich case (Woitke 2000), depending on the gas density. This time scale usually exceeds the cooling and chemical time scales discussed above.

Hydrodynamical time scale. The expansion time scale r/v is found to be large, typically ≈ 12 years at $3\,R_* \approx 2.8\cdot 10^{14}\mathrm{cm}$.

Summarizing these estimates, the hydrodynamical processes, i. e. the gravitational forces and the acceleration of the dust/gas mixture by radiation pressure can be identified as the slowest processes, at least one order of magnitude slower than the radiative transfer, thermal, chemical and dust formation processes considered in this paper and sketched in Fig. 1. Consequently, the expanding wind seems to provide a slowly changing frame, wherein other (faster) processes have sufficient time to interact with each other and to amplify internal perturbations. Such an approximately "closed" control loop of internal feedbacks has been identified in Sect. 2 and discussed in the Sects. 3 and 4. Among the physical processes constituting this control loop, the dust formation is likely to be the slowest process and, hence, is expected to determine the growth time scale of the perturbations.

But of course, possible interrelations with hydrodynamical processes cannot be excluded. Interesting questions arise especially when asking for possible hydrodynamical consequences of a once existing cloudy dust structure. Some of these questions, which clearly go beyond the scope of this paper, are summarized below.

- Does the radiative/thermal instability investigated in this paper interfere with other known dynamical instabilities (see e. g. Inogamov 1999)? What is, for example, the role of propagating shock waves caused by a pulsation of the central star which might induce Rayleigh-Taylor instabilities?
- If the temperature in the shadowed regions behind the opaque dust clouds is in fact lower than in the in-between situated, illuminated regions (see Fig. 3), does the outer pressure compress the gas in these shadowed regions, causing a density contrast?
- Are the opaque structures confined by radiation pressure? If the radiative flux preferentially escapes through the optically thin parts, the radial component of the flux is smaller in the shadowed regions as compared to the inner edges of the clouds. In this case, the dust cloud is expected to be pushed from the star side and the gas density inside the cloud might increase which could facilitate further dust formation.
- Is the hydrodynamical process of dust cloud acceleration in an expanding wind flow dynamically stable?

6. Conclusions

The thermal/radiative stability of astrophysical gases under the influence of a distant source of radiation has been investigated in the grey approximation. The medium is found to be possibly unstable if it possesses a strongly temperature-dependent

opacity with $\frac{\partial \kappa}{\partial T} < 0$ in radiative equilibrium and if it is capable to achieve considerable optical depths by chemical processing. Both preconditions are fulfilled in dust forming gases. The proposed instability arises from (a) the extremely temperature-sensitive source of opacity in combination with (b) multidimensional radiative transfer effects.

Small initial fluctuations of the density and/or temperature structure in a dust forming medium will naturally result in likewise small fluctuations in the forming dust component. An emerging dust shell in the wind of a red giant is therefore not expected to be perfectly spherical symmetric at the time of its formation, but will already possess an internal, slightly patchy, spatial structure. The more opaque parts of this shell will block the outward directed radiation from the central star, while the radiative flux preferentially escapes through the in-between situated, optically thinner parts. Therefore, the more opaque parts will be accompanied by shadowed regions behind them. In these shadows, the temperature of the medium decreases faster than in the neighboring, more illuminated parts. Since the medium is close to the borderline where the temperature is just sufficiently low to become favorable for dust formation, a slight temperature decrease can strongly improve the conditions for subsequent dust formation and growth. Thus, the formation of dust will be accelerated in the shadowed, cooler regions and will be slowed down or even hindered in the illuminated, warmer regions, i. e. the spatial contrast of the degree of condensation will increase.

Such a physical system is self-amplifying, i. e. intrinsically unstable against various kinds of spatial perturbations of an initially homogeneous dust structure. The paper has considered in detail large-scale homogeneous perturbations of a spherically symmetric opacity structure taken from a stationary dust-driven wind model for a carbon star. Radial perturbation modes ($\boldsymbol{k} \parallel \boldsymbol{r}_0$) are thereby found to be stable, whereas perpendicular perturbations ($\boldsymbol{k} \perp \boldsymbol{r}_0$) are found to be unstable in the outer parts of the dust formation / wind acceleration zone. This finding is consistent with the nature of the instability described above, which requires the formation of shadowed regions.

As a possible consequence of this instability, self-organization processes (also termed as structure or domain formation) can be initiated in dust forming media, for example in the winds of red giants. The proposed instability is in particular expected to be involved in the formation of the irregular, cloudy dust structures observed around the infrared carbon star IRC+10216. According to the model, the characteristic time scale for the formation of such structures is determined by the speed of the dust formation process itself. The spatial extent of the emerging dust clouds is expected to correspond to an optical depth $\Delta\tau \gtrsim 1$ at the time of their formation, which is a necessary precondition for the instability. Open questions remain especially when regarding possible interrelations with hydrodynamical processes. More detailed investigations are required here, which must combine time-dependent, hydrodynamical models of the dust formation process with radiative transfer calculations in more than one spatial dimension.

Acknowledgements. The authors would like to thank Dr. Christiane Helling and Heike Richter for their comments on the manuscript. This work has been supported by the DFG, Sonderforschungsbereich 555, Komplexe Nichtlineare Prozesse, Teilprojekt A3, and by the DAAD in the PROCOPE program under grant D/9822849 and 99001.

References

Diamond P.J., Kemball A.J., 1999, In: Le Bertre T., Lèbre A., Waelkens C. (eds.) IAU Symp. 191, AGB stars. ASP Conf. Ser., p. 195
Dominik C., Gail H.-P., Sedlmayr E., Winters J.M., 1990, A&A 240, 365
Gail H.-P., Sedlmayr E., 1988, A&A 206, 153
Gail H.-P., Keller R., Sedlmayr E., 1984, A&A 133, 320
Haniff C.A., Buscher D.F., 1998, A&A 334, L5
Inogamov N.A., 1999, Astrophysics and Space Physics Reviews Vol. 10, Part 2
Lopez B., 1999, In: Le Bertre T., Lèbre A., Waelkens C. (eds.) IAU Symp. 191, AGB stars. ASP Conf. Ser., p. 409
Mihalas D., 1978, Stellar Atmospheres. 2nd ed., W.H. Freeman and Company
Mihalas D., Weibel Mihalas B., 1984, Foundations of Radiation Hydrodynamics. Oxford University Press
Neufeld D.A., Hollenbach D.J., 1994, ApJ 428, 170
Patzer A.B.C., Helling Ch., Winters J.M., Sedlmayr E., 1999, AG Abstr. Ser. 15, 107
Spiegel E.A., 1957, ApJ 126, 202
Trujillo Bueno J., Kneer F., 1990, A&A 232, 135
Tuthill P., Monnier J., Danchi W., Lopez B., 2000, accepted by ApJ
Weigelt G., Balega Y., Blöcker T., et al., 1998, A&A 333, L51
Winters J.M., Dominik C., Sedlmayr E., 1994, A&A 288, 255
Woitke P., 2000, In: Diehl R., Hartmann D. (eds.) Astronomy with Radioactivities. MPE Report 274, Schloß Ringberg, Germany, p. 163
Woitke P., Krüger D., Sedlmayr E., 1996, A&A 311, 927